British Journal of Pharmacology

DOI:10.1111/bph.13285
www.brjpharmacol.org

RESEARCH PAPER

Early treatment with atorvastatin exerts parenchymal and vascular protective effects in experimental cerebral ischaemia

C Potey[1], T Ouk[1], O Petrault[1], M Petrault[1], V Berezowski[1], J Salleron[2], R Bordet[1] and S Gautier[1]

[1]U1171 – Medical Pharmacology Department, Faculty of Medicine, University of Lille 2 – Lille University Hospital, Lille, France, and [2]EA2694 – Biostatistics Department, Faculty of Medicine, University of Lille 2 – Lille University Hospital, Lille, France

Correspondence
Sophie Gautier, U1171 – Medical Pharmacology Department, Faculty of Medicine, University of Lille 2 – Lille University Hospital, Lille, France.
E-mail: sophie.gautier@chru-lille.fr

Received
11 March 2015
Revised
6 August 2015
Accepted
10 August 2015

BACKGROUND AND PURPOSE

From the clinical and experimental data available, statins appear to be interesting drug candidates for preventive neuroprotection in ischaemic stroke. However, their acute protective effect is, as yet, unconfirmed.

EXPERIMENTAL APPROACH

Male C57Bl6/JRj mice were subjected to middle cerebral artery occlusion and treated acutely with atorvastatin (10–20 mg·kg^{-1} day^{-1}; 24 or 72 h). Functional recovery (neuroscore, forelimb gripping strength and adhesive removal test) was assessed during follow-up and lesion volume measured at the end. Vasoreactivity of the middle cerebral artery (MCA), type IV collagen and FITC-dextran distribution were evaluated to assess macrovascular and microvascular protection. Activated microglia, leucocyte adhesion and infiltration were chosen as markers of inflammation.

KEY RESULTS

Acute treatment with atorvastatin provided parenchymal and cerebral protection only at the higher dose of 20 mg·kg^{-1}·day^{-1}. In this treatment group, functional recovery was ameliorated, and lesion volumes were reduced as early as 24 h after experimental stroke. This was associated with vascular protection as endothelial function of the MCA and the density and patency of the microvascular network were preserved. Acute atorvastatin administration also induced an anti-inflammatory effect in association with parenchymal and vascular mechanisms; it reduced microglial activation, and decreased leucocyte adhesion and infiltration.

CONCLUSIONS AND IMPLICATIONS

Acute atorvastatin provides global cerebral protection, but only at the higher dose of 20 mg·kg^{-1}·day^{-1}; this was associated with a reduction in inflammation in both vascular and parenchymal compartments. Our results suggest that atorvastatin could also be beneficial when administered early after stroke.

Abbreviations

AT, atorvastatin; IR, ischaemia-reperfusion; MCA, middle cerebral artery; MCAO, middle cerebral artery occlusion; Phe, phenylephrine

Tables of Links

TARGETS
MPO

LIGANDS			
Atorvastatin	ED1	ICAM-1	VCAM
CCh	H202	Phenylephrine	

These Tables list key protein targets and ligands in this article which are hyperlinked to corresponding entries in http://www.guidetopharmacology.org, the common portal for data from the IUPHAR/BPS Guide to PHARMACOLOGY (Pawson *et al.*, 2014) and are permanently archived in the Concise Guide to PHARMACOLOGY 2013/14 (Alexander *et al.*, 2013).

Introduction

Among the numerous pharmacological strategies that have been evaluated in ischaemic stroke, statins, or HMGCoA-reductase inhibitors, appear as interesting candidates for preventive neuroprotection. Clinical data support a dual beneficial effect in stroke patients, reducing both frequency and severity. The Stroke Prevention with Aggressive Reductions in Cholesterol Levels study first reported a reduction in stroke incidence in secondary prevention (Amarenco *et al.*, 2006). Other studies have since also reported a positive effect on stroke incidence in primary prevention, and a reduction in stroke-related disability and mortality (Ni Chroinin *et al.*, 2013). Experimental studies have provided insights into the underlying mechanisms involved and shown that statins are beneficial due to a pleiotropic mechanism of action. This allows them to act on multiple targets at the same time, resulting in a wide effect on the neurogliovascular unit (Yanuck *et al.*, 2012). Their preventive effect results from the modulation of various pathophysiological pathways, such as excitotoxicity, oxidative stress and inflammation, and is associated with a reduction in both neurological and sensory-motor deficits (García-Bonilla *et al.*, 2012).

Moreover, statin withdrawal at the acute phase has been linked to a negative effect on stroke recurrence, to poorer outcomes and to an increased risk of death (Rodríguez-Yáñez *et al.*, 2008; Flint *et al.*, 2012a). Preclinical studies support the hypothesis of a detrimental impact of statin withdrawal via a rebound effect, the discontinuation of the treatment leading to a worsened outcome (Jasińska-Stroschein *et al.*, 2011). In contrast the in-hospital continuation or the early initiation of a statin treatment is associated with a better chance of survival and a better outcome (Flint *et al.*, 2012a,b), suggesting an acute effect in addition to its well-known preventive, protective effect. Whether the same mechanisms are involved in both the preventive and acute effects is still unclear.

There are scant data regarding the effect of statins administered during the acute phase of ischaemic stroke. Also, the preclinical evidence for a protective effect when the statin treatment is initiated after experimental stroke is limited, the benefits being less obvious than in a preventive setting (García-Bonilla *et al.*, 2012). The underlying pathways and targets providing cerebral protection are still poorly understood. Clinical trials are currently ongoing and will provide insights into its effects on stroke patients, namely the NeuSTART2 (NCT01976936) and the STARS07 (NCT01073007) trials. Therefore, the present study was designed to assess the protective effects of atorvastatin at the acute phase of cerebral ischaemia, from a functional, parenchymal and vascular point of view, focusing on the involvement of underlying inflammation-driven mechanisms.

Methods

Animals

All experiments were performed in strict accordance with the Ethical Committee in Animal Experimentation of Nord-Pas-de-Calais (C2EA-75) and the European Union directive 2010/63/UE (agreement number 00455.02). The experiments are reported in accordance with the ARRIVE guidelines for reporting experiments involving animals (Kilkenny *et al.*, 2010; McGrath *et al.*, 2010). Male C57BL/6JRj mice (CERJ, Saint-Genest-en-l'Isle, France), weighing from 27 to 32 g, housed in a temperature-controlled environment with 12 h light/dark cycles and fed *ad libitum* with a normal diet, were used for all experiments. Animals were randomized after surgery. Experimental data were processed by an investigator blinded for group allocation. The study included 27 sham animals – sham groups – and 108 animals subjected to middle cerebral artery occlusion (MCAO) – ischaemia-reperfusion (IR) groups – that underwent the whole protocol (24 or 72 h). This excluded non-ischaemic animals or animals with incomplete infarcts (10 animals: at 24 h, one animal from the IR + Veh group and one from the IR + atorvastatin (AT)10 group; at 72 h, two animals from the IR + Veh group, three from the IR + AT10 group and three from the IR + AT20 group) and animals that died before the end of follow-up (23 animals).

Experimental design

Mice were trained for 4 days before surgery for the adhesive removal test. They were then subjected to MCAO for 1 h. Atorvastatin base (gift from Genfit, France) was diluted in a vehicle solution (0.05% carboxymethyl cellulose, 0.02% Tween-20, sterile water) and administered orally twice a day for 24 or 72 h following experimental stroke, the first dose being given 1 h after the induction of ischaemia. Functional recovery was assessed 24 and 72 h after surgery (14 to 15 animals per group) (Figure 1).

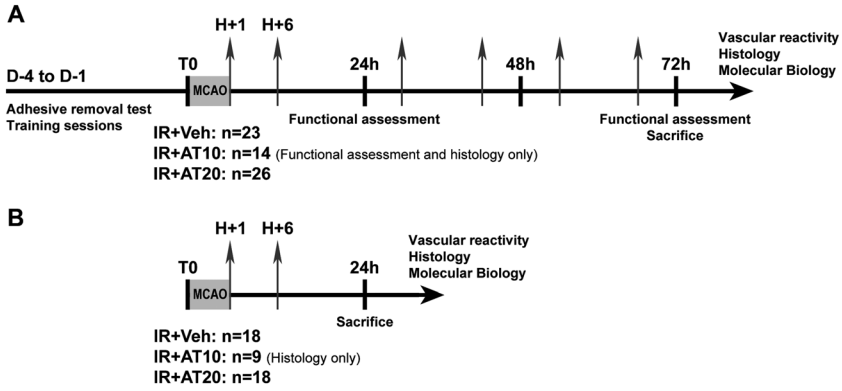

Figure 1

Experimental design. (A) Time course of the 72 h protocol. (B) Time course of the 24 h protocol. The grey arrows represent treatment administrations. Veh, vehicle solution; AT10, atorvastatin 10 mg·kg^{-1}·day^{-1}; AT20, atorvastatin 20 mg·kg^{-1}·day^{-1}.

Middle cerebral artery occlusion model

Transient focal cerebral ischaemia was induced by intraluminal occlusion of the right middle cerebral artery (MCA) as previously described (Ouk *et al.*, 2014a). Animals were anaesthetized with i.p. chloral hydrate (300 mg·kg^{-1}, Sigma-Aldrich, Saint-Quentin Fallavier, France). Occlusion lasted for 60 min, followed by a reperfusion period of 24 or 72 h. Sham-operated animals were subjected to the whole surgical procedure except for the introduction of the occlusive suture. A rectal probe was inserted, and body temperature was maintained at 37 ± 0.5°C with a heating blanket. The right carotid arteries were exposed through a midline cervical incision, and the common carotid and external carotid arteries were ligated with a silk suture. An aneurysm clip was placed across the internal carotid artery, and an arteriotomy was made in the common carotid artery stump, allowing the introduction of a monofilament nylon suture with its tip rounded by heating with a flame. The suture was gently advanced into the internal carotid artery and passed into the intracranial circulatory system into the narrow lumen at the start of the MCA. The occlusion was confirmed by laser-doppler flowmetry (Periflux 5000, Perimed, France). After 60 min, the suture was carefully removed until its tip was blocked by a ligature placed on the common carotid artery to allow reperfusion. Sham animals underwent the same procedure, except for the introduction of the occlusive nylon suture.

Functional assessment

Each test was performed 24 and 72 h after surgery. Mice were placed in the room for 30 min before the beginning of the testing for habituation.

Neurological assessment (adapted from Bederson et al., 1986)

The neurological deficit was scored according to the following scale: 0 = no visible deficit; 1 = flexion of torso and of left forelimb and/or default of extension of left forelimb when held by the tail; 2 = circles towards right when held by the tail, paws on the ground; 3 = falls on left side when walking and/or leans on left side when resting; and 4 = no spontaneous motor activity.

Gripping test

The forelimb gripping strength was measured with an automated grip strength meter (Bioseb, Vitrolles, France). While the mouse was held by the tail, its forepaws were put in contact with a grid connected to the device. It spontaneously tugged the grid, and the corresponding gripping strength was measured. Each animal was maintained in position for 5 s and tested three times with a 5 min interval between each measurement.

Adhesive removal test (adapted from Bouet et al., 2009)

The three parameters assessed in this test were the time to detect tape, giving information on the sensory deficit, and the times to remove the tape from the right (non-altered side) and the left (injured side) forepaws. Mice were placed in a persplex tub for a 60 s habituation period. A piece of adhesive tape (0.4 × 0.4 cm^2, 3 M, Cergy-Pontoise, France) was gently applied to cover the palm of each forepaw. The order of placement (left or right paw first) was alternated in every trial. The animal was then placed back in the tub, and the times to detect and remove the tapes were measured with a maximum limit of 120 s. Mice were trained every day for 4 days before surgery (five trials/session/mouse), to limit the effects of inter-individual variations. At the end of the training period, the animals that could not take off both tapes within 10 s were excluded from the study (two mice overall). The other animals removed the tape from both forepaws in comparable times before MCAO (left side: 5.00 ± 2.71 s; right side: 5.23 ± 2.64 s; $P = 0.656$).

Tissue preparation

Animals were killed 24 or 72 h after MCAO with an overdose of pentobarbital (200 mg·kg^{-1}, i.p.). For the *ex vivo* vascular reactivity study, brains were quickly harvested, and the right MCAwas excised. Brains were then frozen in isopentane and cut later for infarct confirmation. No quantification was

made on these unprocessed tissues. For the molecular biology study, brains were quickly removed, snap frozen in liquid nitrogen and stored at −80°C. For histological studies, animals received an intracardiac infusion with a heparin-treated saline solution and 4% paraformaldehyde (PFA). Brains were removed, post-fixed for 4 h at 4°C in PFA, cryoprotected overnight in sucrose 30%, and finally frozen by immersion in isopentane and stored at −30°C.

Vascular reactivity

Ex vivo vasoreactivity was assessed in a Halpern arteriograph (Living System Instrumentation, Burlington, USA) on a proximal segment of the right MCA, perfused with an oxygenated Krebs solution (pH = 7.4) kept at 37°C. The artery segment was left to stabilize for 1 h at an intraluminal pressure of 20 mmHg. After preconstriction with phenylephrine (Phe) 10^{-4} M, the dose–response curve to CCh was determined by stepwise cumulative addition from 10^{-9} to 10^{-4} M (Sigma-Aldrich, Saint-Genest-en-l'Isle, France). The viability of the artery was verified at the end of the experiment with SNP 10^{-4} M (Sigma-Aldrich, Saint-Genest-en-l'Isle, France). Results are expressed as % increase compared with the preconstricted artery diameter, using the following equation: % relaxation = (Diameter $_{CCh}$ − Diameter $_{Phe}$)/(Diameter $_{basal}$ − Diameter $_{Phe}$) × 100. EC_{50}s for CCh were calculated using GraphPad Prism 5.0 (GraphPad Software, San Diego, USA).

Infarct volume quantification

Twenty micrometre thick cryostat-cut slices were stained with cresyl violet (Sigma-Aldrich, Saint-Genest-en-l'Isle, France). Unstained areas were defined as infarct zones. Total, cortical and striatal lesion volumes were quantified by calculating the numerical integration of the infarcted areas on 12 successive levels using ImageJ software (Image J v.1.47a, NIH, Bethesda, USA). Infarct volumes were corrected to compensate for the oedema, according to the following formula: corrected infarct volume = measured infarct volume × (volume of left hemisphere/volume of right hemisphere).

Immunohistochemistry – colorimetric method

After inhibition of endogenous peroxidases (30 min in methanol, H_2O_2 and PBS), non-specific interaction sites were blocked with normal serum 10% for 1 h. Then, 14 μm thick cryostat-cut slices were left in contact with the primary antibody overnight at 4°C: anti-myeloperoxidase, 1:500 (DAKO, Courtaboeuf, France); anti-ICAM-1, 1:200 (Proteintech, Manchester, UK); anti-ED1, 1:200 (Abcam, Cambridge, UK), and then incubated for 3 h with the secondary antibody at room temperature: anti-rabbit or anti-goat polyclonal antibody, 1:500. Slices were then exposed to an avidin/biotin enzyme complex (ABC kit, Vector, Burlingame, USA). The staining was revealed by DAB/H_2O_2 exposure according to the manufacturer's instructions (Fast DAB Tablets Set, Sigma-Aldrich, Saint-Quentin Fallavier, France). The number of marked vessels (ICAM-1) and cells (MPO, ED1) were counted on three successive slices in four predetermined areas of 1 mm^2 located in the ischaemic zone, including cortex and striatum, for ICAM-1 and MPO, and in the boundaries of the ischaemic zone for ED1. The software ImageJ (NIH) was used for all quantifications. The evaluator was blinded to the treatment status of the evaluated samples (five animals per group).

Immunofluorescence

After simultaneously blocking non-specific interaction sites and of permeabilization with horse serum 10% and 0.3% Triton X-100 in KPBS, 14 μm thick cryostat-cut slices were incubated overnight with the primary antibody at 4°C: anti-type IV collagen, 1:200 (Abcam), then with the secondary antibody: Alexa Fluor anti-rabbit polyclonal antibody, 1:500 (Invitrogen, Cergy, France) for an hour at room temperature. Slides were mounted with Vectashield DAPI (Vector). Type IV collagen is a major constituent of the basal lamina of blood vessels and is used here as a marker for the density of cerebral blood vessels. The fluorescence intensities were read on a confocal microscope (LSM710, Zeiss, Le Pecq, France), and the images were acquired with ZEN 2012 software (Zeiss) retaining the same parameters for each acquisition. The scanned area was 3.60 mm^2, and the final image was obtained combining a z-stack to a tile scan. Images were processed to obtain the maximum intensity projection image. The mean area occupied by the staining was measured using ImageJ on the maximum intensity projection images, keeping the same threshold for each measurement. The evaluator was blinded to the treatment status of the evaluated samples (five animals per group).

Microvascular patency

Mice were injected i.v. with 100 μL of a solution of FITC-dextran (2000 kDa, 10 mg mL^{-1}) (Sigma-Aldrich, Saint-Quentin Fallavier, France). After 2 min, mice were decapitated. Brains were post-fixed in 4% PFA for 24 h at 4°C, embedded in OCT and frozen in liquid nitrogen; 40 μm slices were cryostat-cut and mounted with Vectashield DAPI (Vector). Due to its significant MW, FITC-dextran can only be distributed through patent microvessels, thus allowing them to be visualized under the appropriate wavelength. Images were acquired on a fluorescence microscope (DMIRE2, Leica, Nanterre, France) using the software MetaMorph (v. 1.5.0, Leica).

Gene expression analysis

Brain microvessels isolation

Brain hemispheres were gently grinded with a Dounce homogenizer in ice-cold PBS and treated according to the method previously described by Guo and colleagues (Guo *et al.*, 2010). The cerebral vessels collected were stored at −80°C.

Reverse transcription-PCR

Brain vessel fractions were homogenized in Extract-All buffer (Eurobio, Courtaboeuf, France) with a mechanical grinder, and total RNA was extracted from the samples according to the manufacturer's protocol. Quantitative PCR was performed using a Light Cycler system (Roche Applied Science, Meylan, France) according to the manufacturer's instructions using Light Cycler-FastStart DNA Master SYBR Green mix (Roche Applied Science). The protocol consisted

of a hot start step (8 min at 95°C) followed by 45 cycles including a 10 s annealing step at 60°C and a 10 s elongation step at 72°C. To confirm amplification specificity, the PCR products were subjected to a melting curve analysis. Quantification data represent the mean of three experiments from six animals in each group. TATA-Box Binding Protein (TBP) was selected among other housekeeping genes for normalization in real-time PCR analysis. The sequences of the primers are as follows: TBP up 5′-GGCGGTTTGGCTAGGTTT-3′, low 5′-GGGTTATCTTCACACACCATGA-3′; ICAM-1 up 5′-GGCCACCATCCTGTTCTG-3′, low 5′-TGGTAGACAGCATTTACCCTCA-3′.

Statistical analysis

All tests were performed using SPSS 20.0 (SPSS Inc, Chicago, USA). The threshold for statistical significance was set to $P < 0.05$. Means were compared with one-way ANOVA, or medians by a Kruskal–Wallis test if data were not normally distributed. Data obtained from the functional tests were compared by repeated measures ANOVA. If significance was reached, differences between groups were evaluated with a *post hoc* analysis, using Bonferroni corrected *post hoc* tests following ANOVA, or the Mann–Whitney *U*-test following a non-parametric analysis.

Results

Effect of acute atorvastatin treatment on functional recovery following experimental stroke

The global neurological deficit decreased over time, and atorvastatin (AT) had a significant effect at the dose of 20 mg·kg^{-1} ($F_{(1,41)} = 6.18$; $P = 0.004$). Scores were significantly lower in the IR + AT20 group than in the IR + Veh and IR + AT10 groups (Figure 2A). The forelimb gripping strength increased over time and was also significantly higher in the IR + AT20 group ($F_{(1,41)} = 9.16$; $P < 0.001$) at the two time points 24 and 72 h (Figure 2B). In the adhesive removal test, 24 h after cerebral ischaemia, there was no difference between groups. After 72 h, the IR + AT20 group performed better, and detection times were significantly shorter (Figure 2C – $F_{(1,41)} = 4.21$; $P = 0.022$). AT20-treated mice were also able to remove the piece of tape stuck on the left forepaw faster (Figure 2D – $F_{(1,41)} = 3.90$; $P = 0.028$). In sham-operated mice, the atorvastatin treatment had no effect on the performances (data not shown).

Total, cortical and striatal infarct volumes were significantly reduced in the IR + AT20 group after 24 h when compared with the IR + AT10 and IR + Veh groups ($F_{(2,23)} = 6.91$; $P = 0.004$). The oedema was reduced in a dose-dependent manner in treated animals (Figure 2E). After 72 h of treatment, a significant reduction in the total and cortical infarcts was still observed in the IR + AT20 group ($F_{(2,26)} = 5.53$; $P = 0.010$). Striatal lesion volumes did not differ significantly, and only the oedema was significantly reduced in the IR + AT20 group (Figure 2F).

Effects of acute atorvastatin on the vascular compartment: study of post-ischaemic endothelial dysfunction

Given the lack of effect of the 10 mg·kg^{-1} dose, we decided to carry on the study using only the 20 mg·kg^{-1} dose that provides effective cerebral protection. There was no difference in Phe-induced contractile responses in the four groups, the myogenic tone was not impaired and responses to SNP were comparable (Table 1). Following IR, the endothelial relaxing response induced by CCh was strongly impaired in the vehicle-treated animals (IR + Veh groups; Figure 3A and B). Treatment with atorvastatin briskly reduced the post-ischaemic endothelial dysfunction, significantly restoring the relaxing capacity in the IR + AT20 group within 24 h (Figure 3A). The effect persisted at 72 h (Figure 3B). The maximal response to CCh for these animals was significantly higher than in vehicle-treated animals, and similar to sham groups when compared with the IR + Veh groups (Table 1; $P < 10^{-4}$ at the two time points). Atorvastatin also restored the sensitivity to cholinergic stimulation after 72 h of treatment (Table 2). The EC_{50} values for CCh were significantly smaller in the IR + AT20 groups and comparable with sham groups ($P < 10^{-4}$), whereas the EC_{50} in the IR + Veh group was more than 50-fold higher. In contrast to the IR groups, we did not observe any effect of the atorvastatin treatment on sham-operated animals; it did not modify the endothelial response and sensitivity to CCh in these groups.

Effects of acute atorvastatin on the vascular compartment: study of the microvascular network

The semi-quantitative analysis of the immunofluorescent staining for type IV collagen revealed that there was no difference in the mean stained areas at 24 h. After 72 h of reperfusion, IR + AT20 mice exhibited a higher proportion of stained blood vessels (Figure 3C).

The microvascular distribution of FITC-dextran was reduced in ischaemic conditions, revealing a loss of microvascular patency. In treated animals, FITC-dextran was distributed more extensively through the microvascular network (Figure 3D). Occasional capillary leakage was also observed and was not modified by the treatment.

Evaluation of the acute anti-inflammatory effect of atorvastatin on the parenchymal and vascular compartments

Following 72 h of IR, ED1-positive cells could be detected in the surroundings of the ischaemic area. The number of activated microglial cells was significantly lower in the IR + AT20 group ($U = 0.00$; $P = 0.0079$), giving evidence of a reduction of microglial activation in these animals (Figure 4A).

The parenchymal infiltration of polymorphonuclear neutrophils was drastically diminished after 24 h (Figure 4B; $U = 3.00$; $P = 0.0303$). At the vascular level, the expression of ICAM-1 was significantly reduced in the IR + AT20 group (Figure 4C; U = 0.00; $P = 0.0159$). After 72 h of treatment, there was no difference anymore between treated and untreated animals for both parameters.

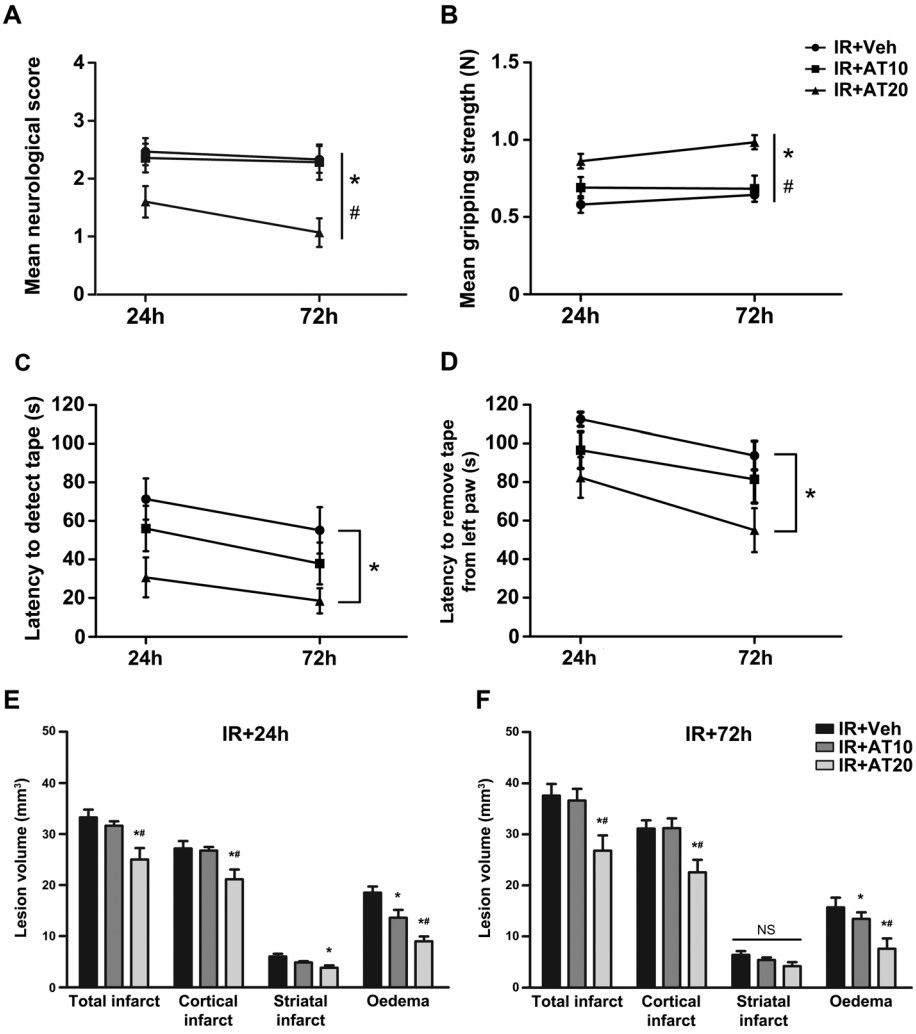

Figure 2

Characterization of the acute neuroprotective effect of atorvastatin. (A) The neurological deficits were significantly reduced in animals treated at the higher dose of 20 mg·kg^{-1}·day^{-1} 24 and 72 h after ischaemia. (B) Atorvastatin 20 mg·kg^{-1}·day^{-1} improved the forelimb gripping strength after 24 and 72 h of reperfusion. (C and D) The sensory-motor deficit is reduced at 72 h after ischaemia in the IR + AT20 group as seen in the adhesive removal test: the latencies to detect (C) and to remove (D) tape from the left forepaw were significantly reduced. IR + Veh: $n = 15$; IR + AT10: $n = 14$; IR + AT20: $n = 15$. (E) In parallel, infarct and oedema volumes were smaller in the IR + AT20 group at 24 h. IR + Veh: $n = 8$; IR + AT10: $n = 9$; IR + AT20: $n = 8$. (F) The effect was still observed at 72 h after ischaemia. IR + Veh: $n = 9$; IR + AT10: $n = 9$; IR + AT20: $n = 10$. Values are expressed as mean ± SEM. *$P < 0.05$ versus IR + Veh group; #$P < 0.05$ versus IR + AT10 group.

Discussion

We showed here that the acute administration of atorvastatin induces parenchymal and vascular protection following experimental stroke. These combined effects result in an improvement in functional recovery. The modulation of inflammation-dependent pathways holds a major place here, contributing to the global cerebral protection we observed.

The significant and early improvement of functional recovery, associated with a reduction in infarct volumes, asserts the global protective effect of acute atorvastatin, linking the cellular protection to a positive motor and sensory impact. Interestingly, this positive impact consisted of short-term effects, including a reduction of the global neurological deficit being seen as early as 24 h post-stroke, and mid-term effects arising at 72 h, like the reduction in sensory-motor deficits evaluated by the adhesive removal test. There are limited data showing the effect of an early statin treatment on the sensory-motor deficits following experimental stroke. Beginning the treatment simultaneously or in the hours following reperfusion induced a reduction in the neurological deficit 24 h later (Céspedes-Rubio *et al.*, 2010; Cui *et al.*, 2010). The effect of a statin treatment started later, that is 24 to 72 h after experimental stroke, is better documented and has been shown to improve sensory-motor recovery for up to 28 days without reducing the lesion itself (Shehadah *et al.*, 2010; Kilic *et al.*, 2014). When treatment was initiated even later, 7 days after MCAO, it also helped to reduce cognitive impairment 3 months later (Shimamura *et al.*, 2007). The long-term effects

Table 1

Basal diameters and vasoreactive effects of phenylephrine (Phe), CCh and SNP on the middle cerebral artery following 24 and 72 h of acute treatment with atorvastatin

	24 h				72 h		
	Sham + Veh ***n* = 10**	**Sham + AT20** ***n* = 6**	**IR + Veh** ***n* = 4**	**IR + AT20** ***n* = 4**	**Sham + AT20** ***n* = 6**	**IR + Veh** ***n* = 7**	**IR + AT20** ***n* = 10**
Basal diameter (μm)	109.00 ± 9.03	102.67 ± 15.47	110.25 ± 8.69	95.00 ± 8.12	104.17 ± 20.04	100.43 ± 14.89	105.60 ± 10.31
Phe 10^{-4} M (% constriction)	29.33 ± 4.76	20.90 ± 3.93	31.19 ± 9.72	28.31 ± 6.80	35.56 ± 4.12	44.16 ± 4.14	32.98 ± 5.74
CCh 10^{-4} M (% relaxation)	93.02 ± 6.74*	83.68 ± 4.59*	34.13 ± 8.20	84.30 ± 3.56*	73.72 ± 4.12*	27.52 ± 5.38	81.62 ± 5.61*
SNP 10^{-4} M (% relaxation)	102.56 ± 6.89	87.23 ± 5.91	84.59 ± 11.48	92.15 ± 1.75	89.74 ± 9.67	97.82 ± 7.42	91.43 ± 4.97

*$P < 0.05$ versus IR + Veh.

of early treatment protocols such as ours, providing acute cellular protection and improving recovery, requires a proper evaluation for confirmation.

We chose to use rather high doses of atorvastatin based on the data available at the time we designed our experiment. Our study confirms that high doses, 10 mg·kg^{-1}·day^{-1} or more, are necessary to achieve acute neuroprotection (Céspedes-Rubio *et al.*, 2010; Cui *et al.*, 2010). In addition, high doses appear to be the most effective when the treatment is initiated in the hours following stroke. In contrast, when the treatment is started later, lower doses also seem to be beneficial. Chen and collaborators (2003) showed that low atorvastatin doses, 1 and 3 mg·kg^{-1}·day^{-1}, but not a higher dose of 8 mg·kg^{-1}·day^{-1}, had a beneficial effect when treatment was started 24 h after experimental stroke. In their study, the 8 mg·kg^{-1}·day^{-1} dose was even almost deleterious, obliterating the positive effects on motor recovery, angiogenesis and neurogenesis exerted by the lower doses. These discrepancies with our results suggest that the pleiotropic effects of atorvastatin not only depend on the dose but also on the scheduled administration time of the treatment. Moreover, the administration route may be of importance as the early administration of low doses has been demonstrated to be of benefit when administered i.v. but not i.p. (Prinz *et al.*, 2008).

Of note, the statin treatment also appeared to interact in a dose-dependent manner with recombinant tissular plasminogen activator (rt-PA), the only authorized treatment for the acute phase of ischaemic stroke. Scheitz and collaborators (2014) recently showed that a previous statin treatment was associated with a greater risk for symptomatic intracerebral haemorrhage in rt-PA-treated patients and that the highest doses were not associated with a favourable outcome after 3 months. However, the introduction of a statin treatment at the acute phase of stroke associated with thrombolysis in naive animals seems beneficial and responsible for a reduction in the rate and severity of secondary haemorrhagic events, exerting a synergistic protective effect (Liu *et al.*, 2006; Zhang *et al.*, 2009). Observational studies, although limited methodologically speaking, seem to be in accordance with these findings (Ni Chroinin *et al.*, 2013). The prospective study STARS07 (NCT01073007) has been specifically designed to address this issue and will give precious insight into this issue.

Our study highlights the role of vascular protection in the cerebral protection provided by atorvastatin. Vascular protection is dual and is aimed at preserving (i) the endothelial function, especially of large arteries in charge of the regulation of cerebral perfusion pressure, and (ii) the structure and patency of microvessels enabling energetic and metabolic exchanges between blood, neurons and glia. Atorvastatin targets large resistance arteries, here the MCA, and participates in the restoration of the endothelial function following IR. The benefit of the acute atorvastatin treatment is not related to an effect on the basal tone but rather to a correction of the post-ischaemic endothelial dysfunction. The endothelial effect of statins is well described, but not in the context of an acute neurovascular event. A long-term treatment ameliorates the endothelial-dependent relaxing response to ACh in large resisting arteries in spontaneously hypertensive rats (Suh *et al.*, 2010). Here, we showed for the first time that atorvastatin protects the MCA against post-ischaemic endothelial dysfunction when administered acutely after stroke. In animal models, it has been shown that a preventive statin treatment could increase the cerebral blood flow (CBF) (Endres *et al.*, 1998; Berger *et al.*, 2008) and preserve the aortic endothelial function 24 h after transient MCAO (Kim *et al.*, 2008). In humans, statins seem to ameliorate vasomotor reactivity without markedly modifying the CBF (Giannopoulos *et al.*, 2012). This effect, on the CBF in animals as on vasomotor reactivity in humans, is related to an improvement in endothelial function.

We also observed a structural and functional protective effect at the microvascular level. We chose two different markers: type IV collagen to visualize the architecture of the microvascular network and FITC-dextran to visualize patent microvessels within that network. Structurally speaking, the network appeared equally altered 24 h after experimental stroke in every group, but it appeared denser after

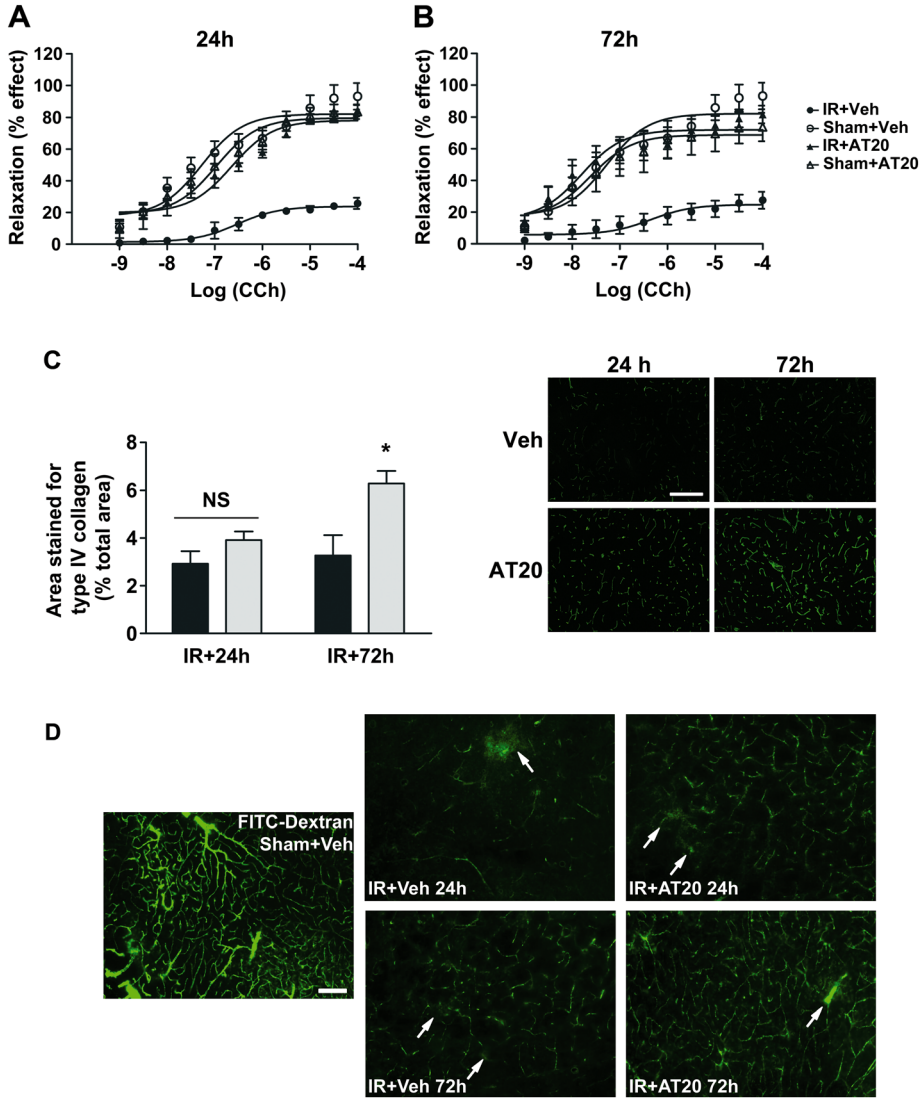

Figure 3

The acute neuroprotective effect of atorvastatin is produced by protection of large and small brain vessels. (A) Dose–response study for the effect of CCh on middle cerebral arteries from sham-operated or ischaemic animals, treated with atorvastatin 20 mg·kg^{-1}·day^{-1} or vehicle, for 24 h. Sham + Veh, $n = 10$; IR + Veh, $n = 4$; Sham + AT20: $n = 6$; IR + AT20, $n = 4$. (B) Dose–response study for the effects of CCh on middle cerebral arteries from sham-operated or ischaemic animals, treated with atorvastatin 20 mg·kg^{-1}·day^{-1} or vehicle, for 72 h. Sham + Veh, $n = 10$; IR + Veh, $n = 7$; Sham + AT20: $n = 6$; IR + AT20, $n = 10$. Results are expressed as the mean % diameter increase in response to CCh normalized to the basal diameter ± SEM. (C) Semi-quantitative analysis of the staining for type IV collagen; stained area expressed as a fraction of the total area and examples of staining are also shown. Results are expressed as median ± interquartile range. $n = 5$ per group. *$P < 0.05$ versus IR + Veh. Bar = 100 μm. (D) Examples of images obtained following the i.v. injection of 2000 kDa FITC-dextran, allowing the visualization of patent microvessels. Arrows indicate capillary leaks. $n = 3$ per group. Bar = 100 μm.

Table 2

Estimated EC_{50} for CCh after 24 and 72 h of an acute treatment with atorvastatin

	Sham + Veh	Sham + AT20	IR + Veh	IR + AT20
24 h	57.99 nM [32.32; 104.60]	73.24 nM [37.34; 143.70]	242.66 nM [108.10; 546.10]	198.61 nM [89.75; 438.90]
72 h		32.79 nM* [12.93; 83.15]	845.28 nM [340.20; 2102.77]	15.76 nM* [6.68; 37.17]

Results are expressed as estimated EC_{50}; 95% confidence interval (parentheses).
*$P < 0.05$ versus IR + Veh.

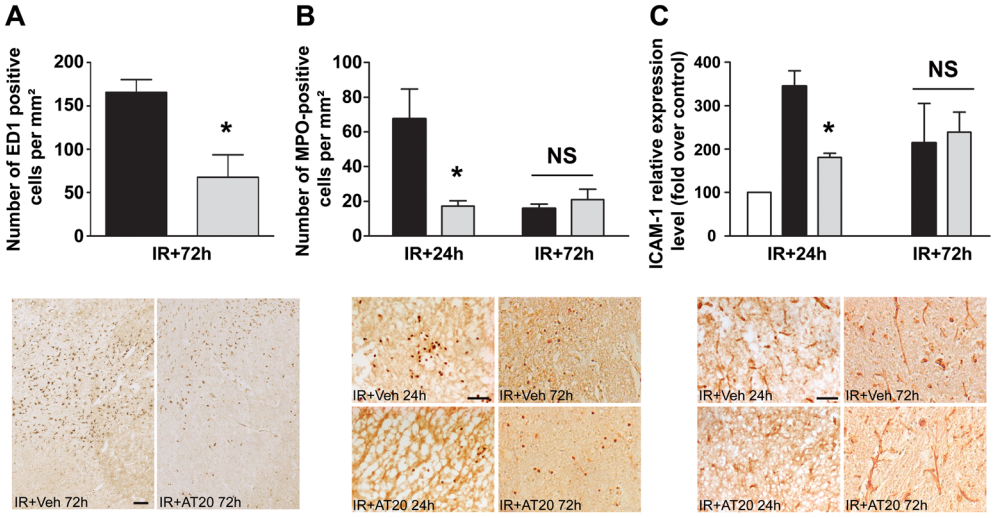

Figure 4

Atorvastatin exerts parenchymal and vascular anti-inflammatory effects. (A) The number of activated microglial cells positive for ED1 was decreased at the periphery of the lesion in atorvastatin-treated animals after 72 h. $n = 5$ per group. Results are presented as median ± interquartile range. Bar = 200 μm. (B) Atorvastatin also reduced the infiltration of polymorphonuclear neutrophils into the injured brain parenchyma. Bar = 50 μm. (C) The quantitative evaluation of the expression of ICAM-1, an endothelial adhesion protein, by reverse transcription-PCR and immunohistochemistry, showed a significant decrease 24 h following ischaemia-reperfusion. Bar = 50 μm. *$P < 0.05$ versus IR + Veh.

72 h in treated animals, implying an effect of atorvastatin on the structure of the microvascular wall. Kawai and collaborators (2011) previously showed that a 4 week preventive treatment with atorvastatin protected brain microvessels, the density of the network being preserved 24 h after MCAO. We also found that microvascular patency was ameliorated. High MW FITC-dextran can only be distributed along with the blood flow in patent, open microvessels. This technique allowed us to show that besides providing structural protection, the acute treatment with atorvastatin also had a functional protective effect on the microvascular network.

In both the macrovascular and microvascular dysfunction occurring after stroke, the establishment of interactions between endothelial cells and neutrophils is involved. In microvessels, the adhesion of neutrophils, and more broadly of leucocytes, contributes to the constitution of microclots impairing the perfusion of regions downstream of these (Greenwood *et al.*, 2011). In arteries, we have previously shown that the adhesion, rolling and infiltration of neutrophils play a major role in the establishment of post-ischaemic endothelial dysfunction (Pétrault *et al.*, 2005). Yet, ICAM-1 and neutrophils can also be looked at from another point of view, not only as markers of vascular injury but more broadly as markers of ongoing inflammatory processes. Inflammatory pathways are activated from the first hours following stroke and will take place in both parenchymatous and vascular compartments (del Zoppo, 2009). The resulting manifestation is polymorphous and evolves over time. Microglial activation is a classic marker for parenchymatous inflammation. Our results are in accordance with the study led by Saito and collaborators (2014), who also found a reduction in microglial activation in rats treated orally with atorvastatin 24 h and 7 days after transient MCAO. Indeed, microglia undergo a series of morphological and functional modifications following ischaemia, characterized by specific patterns of protein expression (Yenari *et al.*, 2010): cytokines, enzymes and chemo-attractant factors, thus participating in tissue injury and promoting leucocyte infiltration and astrocytosis. Leucocytes, here more specifically polymorphonuclear neutrophils, are first attracted towards the lesion and infiltrate throughout the parenchyma to ultimately contribute to the spread of tissue damage. Indeed, the pharmacological depletion of neutrophils is associated with post-stroke protection (Gautier *et al.*, 2009). These neutrophils can infiltrate because of a specific step in the inflammatory reaction taking place in the vascular compartment, which triggers the expression of adhesion molecules in endothelial cells with which leucocytes will interact. We previously showed that a preventive treatment with atorvastatin reduced the expression of ICAM-1 and VCAM following stroke (Ouk *et al.*, 2014a). Hence, it appears that atorvastatin, even administered acutely, exerts a broad acute anti-inflammatory effect affecting both vascular and parenchymatous compartments. We have reasons to believe that the nuclear receptor PPARα is an important pharmacological target underlying this anti-inflammatory effect, as it is activated by statins (Paumelle and Staels, 2008; Ouk *et al.*, 2014a) and its activation induces anti-inflammatory effects (Ouk *et al.*, 2014b).

This study shows that an early atorvastatin treatment provides cerebral protection at the acute phase of stroke leading to tissue protection and improved functional recovery. It emphasizes the importance of neurovascular protection and supports the rationale for the ongoing clinical studies, in which the use of statins at the acute phase of ischaemic stroke are being evaluated.

Acknowledgements

The authors would like to thank Dr Jean-Christophe Devedjian for his useful advice on the molecular biology experiments, Pr Shobu Namura for his guidance on the cerebral blood vessels separation procedure, Meryem Tardivel of the BiCEL facility for access to systems and technical advice and Peter Axerio for his help in correcting this manuscript.

Author contributions

All individuals included as authors of the present paper have contributed substantially and distinctly to the scientific process leading up to the writing of this paper: C. P. performed the research (except for the experiments mentioned later), analysed the data and wrote the article; T. O. and O. P. performed the vasoreactivity experiments; M. P. helped with the surgery; V. B. helped in the microvascular study; J. S. analysed the data coming from the functional assessment; and R. B. and S. G. designed the study and edited the article.

Conflict of interest

None.

References

Alexander SPH, Benson HE, Faccenda E, Pawson AJ, Sharman JL, Spedding M *et al.* (2013). The Concise Guide to PHARMACOLOGY 2013/14: enzymes. Br J Pharmacol 170: 1797–1867.

Amarenco P, Bogousslavsky J, Callahan A, Goldstein LB, Hennerici M, Rudolph AE *et al.* (2006). High-dose atorvastatin after stroke or transient ischemic attack. N Engl J Med 355: 549–59.

Bederson JB, Pitts LH, Tsuji M, Nishimura MC, Davis RL, Bartkowski H (1986). Rat middle cerebral artery occlusion: evaluation of the model and development of a neurologic examination. Stroke 17: 472–6.

Berger C, Xia F, Maurer M, Schwab S (2008). Neuroprotection by pravastatin in acute ischemic stroke in rats. Brain Res Rev 58: 48–56.

Bouet V, Boulouard M, Toutain J, Divoux D, Bernaudin M, Schumann-Bard P *et al.* (2009). The adhesive removal test: a sensitive method to assess sensorimotor deficits in mice. Nat Protoc 4: 1560–1564.

Céspedes-Rubio A, Jurado F, Cardona-Gómez G (2010). p120 catenin/αN-catenin are molecular targets in the neuroprotection and neuronal plasticity mediated by atorvastatin after focal cerebral ischemia. J Neurosci Res 88: 3621–34.

Chen J, Zhang ZG, Li Y, Wang Y, Wang L, Jiang H *et al.* (2003). Statins induce angiogenesis, neurogenesis, and synaptogenesis after stroke. Ann Neurol 53: 743–51.

Cui L, Zhang X, Yang R, Wang L, Liu L, Li M *et al.* (2010). Neuroprotection of early and short-time applying atorvastatin in the acute phase of cerebral ischemia: down-regulated 12/15-LOX, p38MAPK and cPLA2 expression, ameliorated BBB permeability. Brain Res 1325: 164–73.

Endres M, Laufs U, Huang Z, Nakamura T, Huang P, Moskowitz MA *et al.* (1998). Stroke protection by 3-hydroxy-3-methylglutaryl (HMG)-CoA reductase inhibitors mediated by endothelial nitric oxide synthase. Proc Natl Acad Sci 95: 8880–5.

Flint AC, Kamel H, Navi BB, Rao VA, Faigeles BS, Conell C *et al.* (2012a). Inpatient statin use predicts improved ischemic stroke discharge disposition. Neurology 78: 1678–1683.

Flint AC, Kamel H, Navi BB, Rao VA, Faigeles BS, Conell C *et al.* (2012b). Statin use during ischemic stroke hospitalization is strongly associated with improved poststroke survival. Stroke 43: 147–54.

García-Bonilla L, Campos M, Giralt D, Salat D, Chacón P, Hernández-Guillamon M *et al.* (2012). Evidence for the efficacy of statins in animal stroke models: a meta-analysis. J Neurochem 122: 233–43.

Gautier S, Ouk T, Petrault O, Caron J, Bordet R (2009). Neutrophils contribute to intracerebral haemorrhages after treatment with recombinant tissue plasminogen activator following cerebral ischaemia. Br J Pharmacol 156: 673–679.

Giannopoulos S, Katsanos A, Tsivgoulis G, Marshall R (2012). Statins and cerebral hemodynamics. J Cereb Blood Flow Metab 32: 1973–1976.

Greenwood J, Heasman SJ, Alvarez JI, Prat A, Lyck R, Engelhardt B (2011). Review: leucocyte-endothelial cell crosstalk at the blood–brain barrier: a prerequisite for successful immune cell entry to the brain. Neuropathol Appl Neurobiol 37: 24–39.

Guo Q, Wang G, Namura S (2010). Fenofibrate improves cerebral blood flow after middle cerebral artery occlusion in mice. J Cereb Blood Flow Metab 30: 70–8.

Jasińska-Stroschein M, Owczarek J, Wejman I, Orszulak-Michalak D (2011). Novel mechanistic and clinical implications concerning the safety of statin discontinuation. Pharmacol Rep PR 63: 867–879.

Kawai H, Deguchi S, Deguchi K, Yamashita T, Ohta Y, Omote Y *et al.* (2011). Protection against ischemic stroke damage by synergistic treatment with amlodipine plus atorvastatin in Zucker metabolic rat. Brain Res 1382: 308–314.

Kilic E, Reitmeir R, Kilic Ü, Caglayan AB, Beker MC, Kelestemur T *et al.* (2014). HMG-CoA reductase inhibition promotes neurological recovery, peri-lesional tissue remodeling, and contralesional pyramidal tract plasticity after focal cerebral ischemia. Front Cell Neurosci 8: 422.

Kilkenny C, Browne W, Cuthill IC, Emerson M, Altman DG (2010). NC3Rs Reporting Guidelines Working Group. Br J Pharmacol 160: 1577–1579.

Kim H, Sawada N, Soydan G, Lee H, Zhou Z, Hwang S *et al.* (2008). Additive effects of statin and dipyridamole on cerebral blood flow and stroke protection. J Cereb Blood Flow Metab 28: 1285–1293.

Liu X, Zhang Z, Zhang L, Morris D, Kapke A, Lu M *et al.* (2006). Atorvastatin downregulates tissue plasminogen activator-aggravated genes mediating coagulation and vascular permeability in single cerebral endothelial cells captured by laser microdissection. J Cereb Blood Flow Metab 26: 787–796.

McGrath J, Drummond G, McLachlan E, Kilkenny C, Wainwright C (2010). Guidelines for reporting experiments involving animals: the ARRIVE guidelines. Br J Pharmacol 160: 1573–1576.

Ni Chroinin D, Asplund K, Asberg S, Callaly E, Cuadrado-Godia E, Diez-Tejedor E *et al.* (2013). Statin therapy and outcome after ischemic stroke: systematic review and meta-analysis of observational studies and randomized trials. Stroke 44: 448–456.

Ouk T, Potey C, Laprais M, Gautier S, Hanf R, Darteil R *et al.* (2014a). PPARα is involved in the multitargeted effects of a pretreatment with atorvastatin in experimental stroke. Fundam Clin Pharmacol 28: 294–302.

Ouk T, Gautier S, Pétrault M, Montaigne D, Maréchal X, Masse I *et al.* (2014b). Effects of the PPAR-α agonist fenofibrate on acute and short-term consequences of brain ischemia. J Cereb Blood Flow Metab 34: 542–551.

Paumelle R, Staels B (2008). Cross-talk between statins and PPARalpha in cardiovascular diseases: clinical evidence and basic mechanisms. Trends Cardiovasc Med 18: 73–8.

Pawson AJ, Sharman JL, Benson HE, Faccenda E, Alexander SP, Buneman OP *et al.* (2014). The IUPHAR/BPS Guide to PHARMACOLOGY: an expert-driven knowledgebase of drug targets and their ligands. Nucl Acids Res 42 (Database Issue): D1098–106.

Pétrault O, Ouk T, Gautier S, Laprais M, Gelé P, Bastide M *et al.* (2005). Pharmacological neutropenia prevents endothelial dysfunction but not smooth muscle functions impairment induced by middle cerebral artery occlusion. Br J Pharmacol 144: 1051–8.

Prinz V, Laufs U, Gertz K, Kronenberg G, Balkaya M, Leithner C *et al.* (2008). Intravenous rosuvastatin for acute stroke treatment: an animal study. Stroke 39: 433–8.

Rodríguez-Yáñez M, Dávalos A, Castillo J (2008). Withdrawal from statins: implications for secondary stroke prevention and acute treatment. Int J Stroke 3: 85–87.

Saito T, Nito C, Ueda M, Inaba T, Kamiya F, Muraga K *et al.* (2014). Continuous oral administration of atorvastatin ameliorates brain damage after transient focal ischemia in rats. Life Sci 94: 106–114.

Scheitz JF, Seiffge DJ, Tütüncü S, Gensicke H, Audebert HJ, Bonati LH *et al.* (2014). Dose-related effects of statins on symptomatic intracerebral hemorrhage and outcome after thrombolysis for ischemic stroke. Stroke 45: 509–514.

Shehadah A, Chen J, Cui X, Roberts C, Lu M, Chopp M (2010). Combination treatment of experimental stroke with Niaspan and simvastatin, reduces axonal damage and improves functional outcome. J Neurol Sci 294: 107–11.

Shimamura M, Sato N, Sata M, Kurinami H, Takeuchi D, Wakayama K *et al.* (2007). Delayed postischemic treatment with fluvastatin improved cognitive impairment after stroke in rats. Stroke 38: 3251–8.

Suh J, Choi D, Chang H, Cho Y, Youn T, Chae I *et al.* (2010). HMG-CoA reductase inhibitor improves endothelial dysfunction in spontaneous hypertensive rats via down-regulation of caveolin-1 and activation of endothelial nitric oxide synthase. J Kor Med Sci 25: 16–23.

Yanuck D, Mihos C, Santana O (2012). Mechanisms and clinical evidence of the pleiotropic effects of the hydroxy-methyl-glutaryl-CoA reductase inhibitors in central nervous system disorders: a comprehensive review. Int J Neurosci 122: 619–29.

Yenari M, Kauppinen T, Swanson R (2010). Microglial activation in stroke: therapeutic targets. Neurother 7: 378–391.

Zhang L, Chopp M, Jia L, Cui Y, Lu M, Zhang ZG (2009). Atorvastatin extends the therapeutic window for tPA to 6 h after the onset of embolic stroke in rats. J Cereb Blood Flow Metab 29: 1816–24.

del Zoppo GJ (2009). Inflammation and the neurovascular unit in the setting of focal cerebral ischemia. Neuroscience 158: 972–982.